Science of the Total Environment 1030 (2026) 181790

Contents lists available at ScienceDirect

Science of the Total Environment

journal homepage: www.elsevier.com/locate/scitotenv

Local and distal processes determine precipitation isotope records in the Great Plains USA

Saranya Puthalath [a,*], Matthew F. Kirk [b], Rachel M. Keen [c], Alejandro N. Flores [d], Sharon A. Billings [e], Pamela L. Sullivan [f], Jesse B. Nippert [g]

[a] Department of Geology and Division of Biology, Kansas State University, United States of America
[b] Department of Geology, Kansas State University, United States of America
[c] College of Earth, Ocean and Atmospheric Sciences, Oregon State University, United States of America
[d] Department of Geosciences, Boise State University, United States of America
[e] Department of Ecology & Evolutionary Biology and Kansas Biological Survey & Center for Ecological Research, University of Kansas, United States of America
[f] College of Earth, Ocean, and Atmospheric Sciences, Oregon State University, United States of America
[g] Division of Biology, Kansas State University, United States of America

HIGHLIGHTS

- A 22-year (2001–2022) precipitation $\delta^{18}O$ record from the central Great Plains reveals long-term isotope variability.
- Gulf of Mexico moisture via the Great Plains Low-Level Jet strongly influences $\delta^{18}O$ and d-excess despite variable contributions.
- Monthly precipitation $\delta^{18}O$ positively correlates with rainfall amount, temperature, and vapor pressure deficit.
- Extreme wet (2019) and dry (2012) years show combined effects of circulation anomalies and evaporative demand on isotopes.

GRAPHICAL ABSTRACT

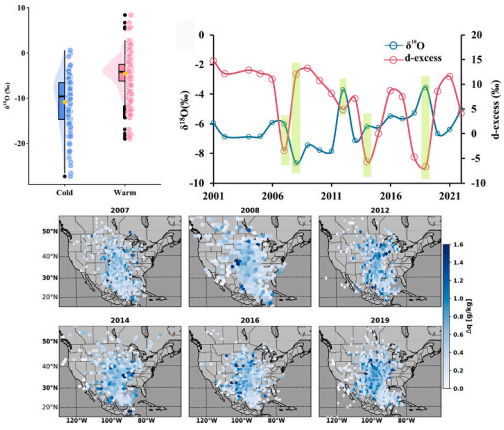

ARTICLE INFO

Keywords:
Isotope hydrology
Moisture recycling
Vapor pressure deficit

ABSTRACT

Nuanced characterizations of moisture source dynamics and local hydrometeorological processes are essential for interpreting long-term records of stable isotopes in precipitation. Here, we analyze over two decades of stable isotope records from a site in the Great Plains of United States, revealing a distinct seasonal contrast in $\delta^{18}O$ variability between warm (March–November) and cold (December–February) periods. During the warm season, isotopic enrichment was largely driven by enhanced convective activity and sub-cloud evaporation under high VPD conditions. Back-trajectory diagnostics indicate that continental moisture sources dominate precipitation at the study site, while Gulf of Mexico transport via the Great Plains low-level jet exerts a disproportionate influence on $\delta^{18}O$ and d-excess variability. During extreme precipitation years, isotopic signatures reflect the combined

* Corresponding author.
E-mail address: saranyaputhalath@ksu.edu (S. Puthalath).

https://doi.org/10.1016/j.scitotenv.2026.181790
Received 20 November 2025; Received in revised form 5 April 2026; Accepted 8 April 2026
Available online 16 April 2026

effects of atmospheric circulation anomalies and local aridity. The 2012 drought year exhibited elevated $\delta^{18}O$ and reduced d-excess consistent with enhanced kinetic fractionation under dry conditions, whereas the wet year 2019 showed isotopic enrichment associated with intensified Gulf-sourced moisture transport under humid conditions. These findings demonstrate how precipitation $\delta^{18}O$ in the Great Plains integrates both local evaporative demand and large-scale moisture transport processes. Given ongoing challenges in representing humidity trends and regional hydroclimate dynamics in climate models, improved characterization of moisture sources and isotope variability is critical for evaluating model projections and interpreting long-term climate change in semi-arid continental regions.

1. Introduction

Changes in atmospheric moisture transport and precipitation dynamics strongly drive climate variability in interior continents. The isotopic composition of precipitation ($\delta^{18}O$ and $\delta^{2}H$) reflects the combined influence of local and large-scale hydrometeorological processes. Classical frameworks describe temperature as the dominant controlling factor in temperate regions, while the amount effect is the dominant controlling factor in the tropics (Dansgaard, 1964; Rozanski et al., 1993). However, beyond the classical temperature or amount effects, precipitation $\delta^{18}O$ is universally influenced by moisture source conditions, moisture transport history, rainout processes, sub-cloud evaporation, and continental moisture recycling (Bedaso and Wu, 2020; Lekshmy et al., 2014; Rahul and Ghosh, 2018; Saranya et al., 2018a). In continental interior locations such as the Great Plains of North America, distal hydrometeorological processes, including advection from oceanic sources and recycled moisture from evapotranspiration, can significantly modulate the precipitation isotope signal (Jasechko et al., 2013; Saranya et al., 2021; Wei et al., 2017). Despite growing recognition of these influences, the relative influences of local versus remote controls on precipitation isotope variability remain poorly constrained across continental interiors, largely due to the lack of long-term observational datasets linking precipitation isotopes with hydrometeorological controls.

Atmospheric dryness or Vapor Pressure Deficit (VPD) provides an additional control on precipitation isotope variability, distinct from temperature effects (Adhikari et al., 2020; Wu et al., 2015). VPD, defined as the difference between saturation and actual vapor pressure, indicates atmospheric evaporative demand (Broz et al., 2021; Ficklin and Novick, 2017) and influences isotopic fractionation through its effects on evaporation and sub-cloud processes (Wu et al., 2018). Elevated VPD indicates unsaturated conditions that enhance sub-cloud evaporation and kinetic fractionation during raindrop descent, enriching precipitation $\delta^{18}O$ (Dansgaard, 1964; Jouzel and Merlivat, 1984). Although these mechanisms are well-established conceptually, the extent to which sub-cloud evaporation and VPD modulate precipitation $\delta^{18}O$ variability at continental scales remain poorly constrained.

The hydroclimate of the Great Plains is determined by a combination of external moisture advection and continental recycling. The Gulf of Mexico supplies a major fraction of the precipitation through the Great Plains low-level jet (Bonner, 1968; Weaver and Nigam, 2011). The region is also one of the most extensively cultivated and irrigated landscapes globally, and hence continental moisture recycling can contribute substantially to total regional precipitation (Deangelis et al., 2010; Sala, 2025). Given the sensitivity of stable water isotopes, $\delta^{18}O$ and $\delta^{2}H$, to both moisture source and transport conditions, these records are well-positioned to document variability in both precipitation and terrestrial climate proxies (Salati et al., 1979; Saranya et al., 2021, 2018b; Xia and Winnick, 2021).

Understanding these controls becomes increasingly important as climate change continues to alter regional hydroclimate. Rising temperatures and atmospheric aridity are projected to increase evaporative demand across the central Great Plains (Ficklin and Novick, 2017), while vegetation shifts such as woody encroachment (Ratajczak et al., 2012; Stevens et al., 2017; Van Auken, 2009; Twidwell et al., 2013) may further modify land-atmosphere feedbacks (Deng et al., 2021; Keen et al., 2024; Sadayappan et al., 2023). As current climate models struggle to capture humidity trends (Simpson et al., 2024), especially in relatively dry regions, an improved understanding of the competing sources of precipitation, their isotope variability, and their long-term dynamics is crucial to evaluate and predict climate model projections.

Here, we address three key questions that are particularly important for understanding hydroclimate dynamics in continental interior regions where multiple moisture sources contribute towards local precipitation: (1) What local hydrometeorological processes control precipitation $\delta^{18}O$ variability? (2) How do oceanic and continental moisture sources partition and vary through time? and (3) To what extent do atmospheric vapor content and moisture-source variability influence precipitation isotope variability? The central Great Plains provides a unique setting to investigate these questions because it lies far from oceanic boundaries yet receives substantial Gulf-sourced moisture while also experiencing strong continental recycling.

To answer these questions, we analyze a 20-year record of weekly precipitation isotope measurements from Konza Prairie Biological Station (KPBS) in northeast Kansas, USA, and combine these observations with back trajectory-based moisture source diagnostics. In addition to long-term variability, we examine isotopic behavior during an anomalously dry and wet year, respectively, to evaluate how circulation anomalies and atmospheric dryness modulate isotope signatures under contrasting hydroclimatic conditions. This integrated framework enables us to quantify moisture source contributions, evaluate their temporal variability, and assess their relationship with precipitation $\delta^{18}O$ in a continental interior setting.

2. Methods

2.1. Study site

The study site, Konza Prairie Biological Station (KPBS, 39°05′N, 96°35′W), is located in the northern Flint Hills region of Kansas, USA. The region is characterized by a temperate continental climate with an average annual precipitation of 811 mm, of which 75% occurs during the growing season (April to October) (Keen et al., 2024). The annual average temperature for KPBS is 11 °C, with the hottest month being July and January being the coldest month. The mean annual cycle of temperature, precipitation amount, VPD, and precipitation $\delta^{18}O$ (Fig. 1) shows a pronounced seasonal contrast. December–February is characterized by low temperatures and low atmospheric evaporative demand, whereas March–November exhibits warmer conditions and higher VPD. These seasonal differences strongly influence precipitation formation and isotopic fractionation processes. $\delta^{18}O$ peaks in July, reflecting the combined influence of multiple warm-season processes, including the annual maxima in temperature and VPD at KPBS. These conditions, along with convective precipitation, are the most proximal explanations for the peak $\delta^{18}O$ in mid-summer (July).

Air masses from the Gulf of Mexico bring oceanic moisture to the region, but their further spread towards the western end of the state is limited due to the increase in land surface elevation (Miller and Appel, 1997). Precipitation and temperature are strongly related at this site, as warmer months are wetter, although this relationship tends to weaken

during extreme drought years (Knapp et al., 2020).

2.2. Sampling, isotopic analysis and data categorization

Weekly bulk precipitation sampling was conducted continuously from January 2001 to November 2022 at the headquarters region of KPBS. A total of 638 precipitation samples were collected using an Ott Pluvio rain gauge utilizing a sensor arm that seals the gauge when dry and opens during precipitation events (Blair, 2023). To avoid the effects of post-precipitation evaporative enrichment, the samples were not exposed to direct radiation. On Tuesday mornings of each week, samples were transferred to polypropylene bottles, sealed with parafilm tape, and then stored in airtight polypropylene containers at 4 °C. Snowfall samples were collected using the same gauge and were allowed to melt prior to transfer to bottles to ensure complete recovery of the total volume. The analysis for water stable isotopes ($\delta^{18}O$ and $\delta^{2}H$) was carried out at the Stable Isotope and Mass Spectrometry Lab (SIMSL) at Kansas State University using a Picarro WS-CRDS water isotope analyzer. Each sample was analyzed using six sequential injections on a Picarro WS-CRDS system, and the average of the final three injections was used for reporting to minimize memory effect and carry over between samples. Instrument calibration was done using a laboratory working standard calibrated against the Vienna Mean Standard Ocean Water (VSMOW). Three internal reference waters spanning a wide isotopic range (KS-enriched: $\delta^{2}H = -2‰$, $\delta^{18}O = 4.1‰$; Evian: $\delta^{2}H = -71‰$, $\delta^{18}O = -9.9‰$; and Eldorado: $\delta^{2}H = -106‰$, $\delta^{18}O = -14.3‰$) were measured throughout each run to normalize sample values and monitor analytical precision and reproducibility. Isotopic values were then expressed in per mil (‰) relative to the VSMOW. The long-term precision of the water isotopic analysis was <0.15‰ for $\delta^{18}O$ and < 0.3‰ for $\delta^{2}H$ (Keen et al., 2024). Additionally, the secondary parameter, deuterium excess (d-excess) = $\delta^{2}H - 8 \times \delta^{18}O$ (Dansgaard, 1964), was calculated to assess moisture source conditions, which can be modified by secondary processes such as evaporation and moisture recycling. Since $\delta^{18}O$ and $\delta^{2}H$ are strongly coupled along the meteoric water line and generally exhibit parallel variability, subsequent analyses focus on $\delta^{18}O$ and d-excess, which together retain the key information contained in $\delta^{2}H$. Using d-excess also provides information about the moisture source conditions, kinetic fractionation, and moisture recycling signatures that might not have been captured with $\delta^{18}O$ and $\delta^{2}H$.

Weekly isotope values were aggregated to monthly values using precipitation amount-weighted averaging to account for variability in event size. Seasonal and annual isotope values were calculated from these monthly amount-weighted means. Although KPBS experiences four distinct meteorological seasons (winter, spring, summer, and fall), the data in this study were grouped into two broad seasonal categories: cold (December–February) and warm (March–November) seasons. This categorization was chosen to highlight the contrasting hydrometeorological regimes that presumably influence the isotopic fractionation processes related to precipitation formation and sub-cloud processes. The cold seasons are characterized by the lowest temperatures, low VPD, and a greater probability of snowfall that reduces sub-cloud evaporation. In contrast, warm seasons are characterized by higher temperatures, elevated VPD, dominance of convective activities, liquid precipitation, and thus greater possibilities for sub-cloud evaporation.

2.3. Identifying dominant moisture uptake regions using HYSPLIT back trajectory model

Back trajectory analyses, an approach that helps determine air mass

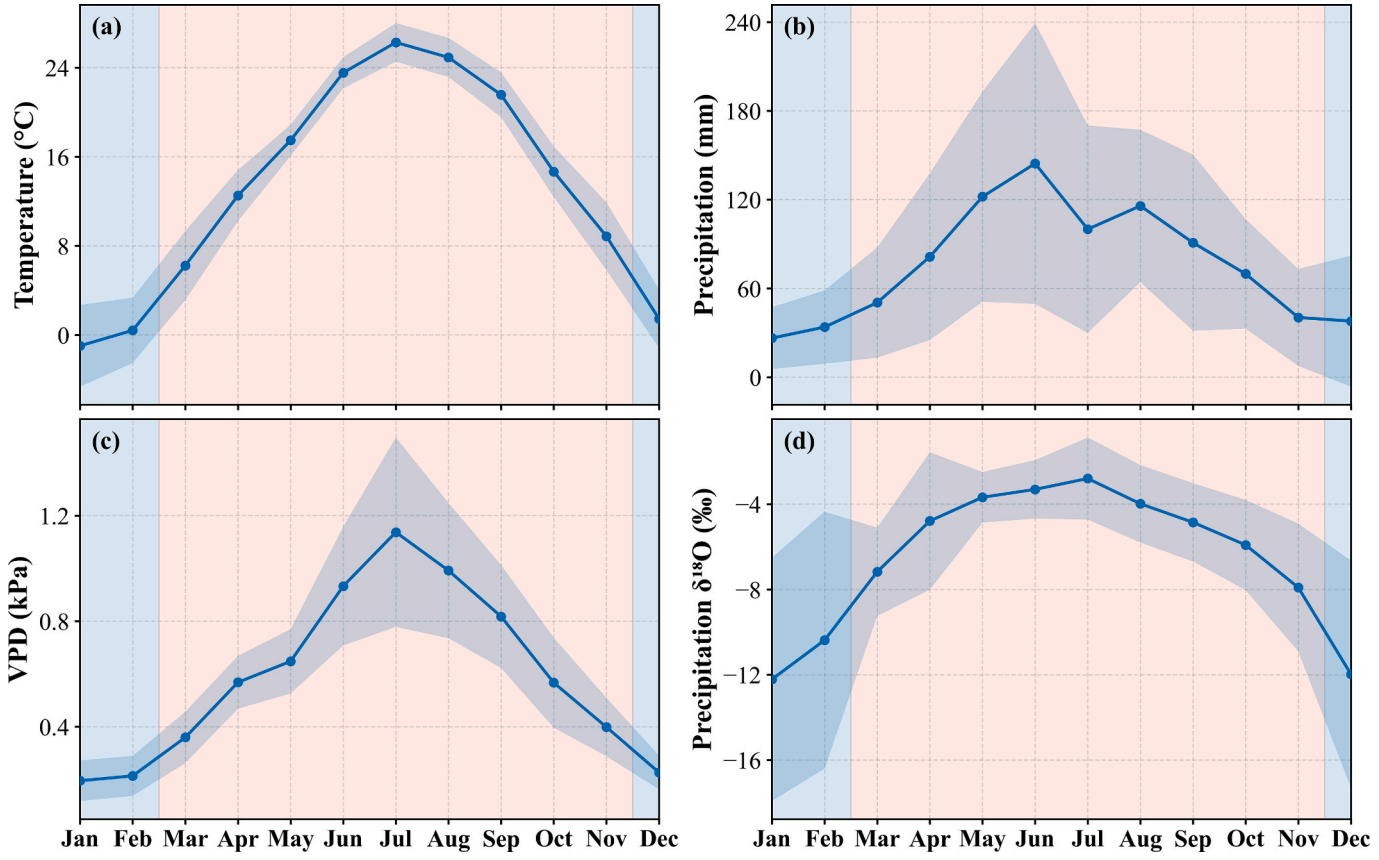

Fig. 1. Mean annual cycle (monthly climatology) of (a) temperature, (b) precipitation, (c) VPD, and (d) $\delta^{18}O$ at KPBS based on the monthly values over the full study period. Solid lines show the climatological monthly mean, and the shaded region around the line indicates interannual variability (±1 SD). Blue background shading highlights the cold season (December–February), whereas red shading indicates the warm season (March–November).

origins (Wernli and Davies, 1997), were done at 6-h intervals with a 72-h backward total run time to evaluate the influence of changing moisture sources on the stable isotope composition of precipitation. For these analyses, we used the NOAA/Air Resources Laboratory (ARL) Hybrid Single-Particle Lagrangian Integrated Trajectory (HYSPLIT) model (Draxler and Hess, 1998; Stein et al., 2015). The 72 h run time was selected to reflect the average moisture residence time in the United States, which is typically less than three days (Trenberth, 1999).

PYSPLIT (Warner, 2018), a python-based library with an embedded moisture uptake algorithm (Sodemann et al., 2008), was used to mass-generate trajectories and perform computations along the trajectory. The moisture uptake algorithm is based on the principle of mass conservation, assuming that increases or decreases in specific humidity along the trajectory were contributed by evaporation or precipitation, respectively (Sodemann, 2025; Sodemann et al., 2008). Only precipitating trajectories were used in the calculation. Since each precipitation sample collected at KPBS represented the integrative signature of the previous seven days, all the precipitating trajectories during these seven days were considered for the computation. The criteria for moisture uptake were chosen based on the previous studies that adopted this diagnostic (Molina et al., 2020; Pfahl et al., 2014; Saranya et al., 2021; Zhang et al., 2023). Based on the back trajectory analysis, four primary moisture source regions contributed to precipitation at KPBS and were selected for further analysis: the Gulf of Mexico, the Great Lakes, the Eastern CONUS, and the Western CONUS (Text S1) (Fig. 2).

Percentage contribution from each source region was estimated following the formula $F_s = ((\Sigma fm/TF) \times R) \times 100$). Where, F_s represents the percentage contribution of moisture from a specific source region (s) along a given trajectory, fm is the fraction of moisture from that source, TF is the total fractional contribution (g/kg) from all source regions, and R is the total precipitation received at the sampling location.

2.4. k-means clustering

To elucidate the hydrometeorological patterns of the $\delta^{18}O$ vs d-excess relationship, k-means clustering was performed (Kanungo et al., 2002). The calculation separated the data into different clusters by minimizing the variance in each cluster. This enabled us to evaluate the different hydro-meteorological processes governing the precipitation isotope records. The choice of three clusters enabled optimum clustering by reducing the sum of squared errors.

2.5. Statistical methods

Relationships between isotopic variables and hydrometeorological parameters were analyzed using Pearson product-moment correlation coefficients (r). Correlation matrices were constructed for monthly amount-weighted and annual datasets, and the statistical significance was assessed using two-tailed tests ($\alpha = 0.05$).

To quantify the relationship between moisture source contributions and precipitation $\delta^{18}O$, simple linear regression analyses were performed. Because each regression included a single predictor, the reported multiple R values are equivalent to Pearson correlation coefficients (r), and associated *p*-values indicate significance of the linear relationship. All statistical analyses were conducted in Python and Microsoft Excel.

2.6. Data sources

The Global Data Assimilation (GDAS) (ftp://arlftp.arlhq.noaa.gov/pub/archives/gdas1) data product was used as input meteorological data in the HYSPLIT model. Total precipitation amount and the convective fraction of precipitation (fraction of total precipitation that is convective) were obtained from the North American Land Data Assimilation System (NLDAS) Phase 2 forcing data (monthly, $0.125^0 \times 0.125^0$) (Xia et al., 2009). The 4-km resolution gridded temperature and VPD

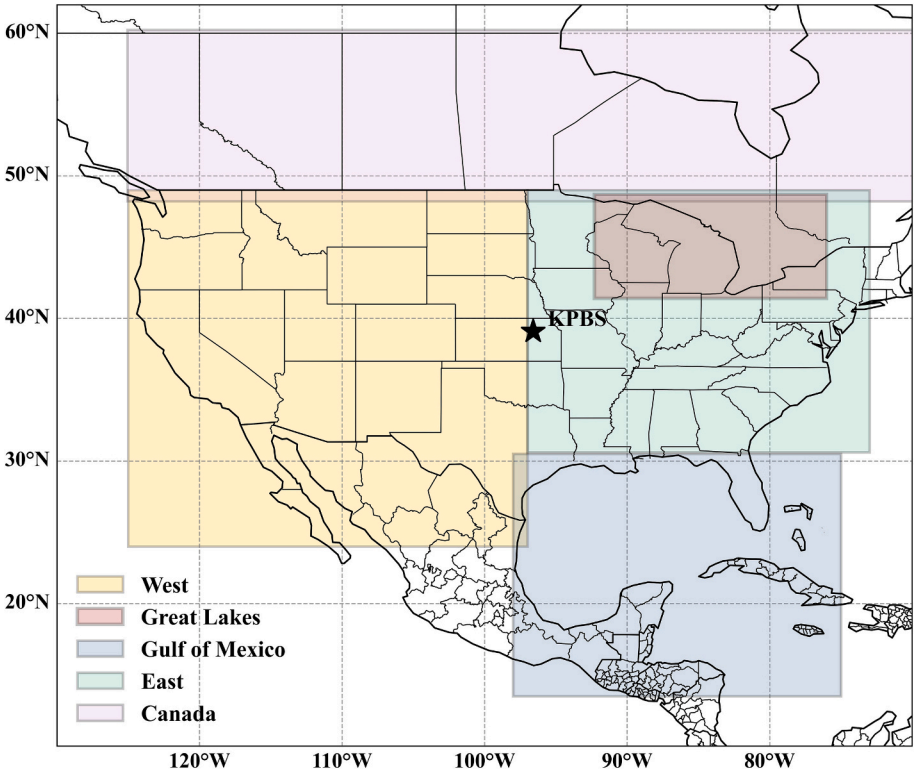

Fig. 2. Geographic definition of moisture source regions used for trajectory-based moisture uptake analysis. Shaded regions indicate the respective moisture sources, and the "star" symbol marks the locations of the Konza Prairie Biological Station (KPBS).

data were obtained from the PRISM Climate Group, Oregon State University (https://prism.oregonstate.edu/). The geopotential height, specific humidity, and wind vector data were obtained from ECMWF's atmospheric reanalysis dataset ERA5. Air temperature and relative humidity were obtained from the meteorological station installed at the KPBS (Nippert et al., 2026). Local VPD was calculated from these measurements as the difference between saturation vapor pressure (SVP) and actual vapor pressure (AVP).

$$SVP = 0.6108^{*}e^{\left(\frac{17.27^{*}T}{T+273.3}\right)}$$

$$AVP = \left(\frac{RH}{100}\right)^{*}SVP$$

$$VPD = SVP - AVP$$

3. Results

In the sections that follow, we examine the isotopic-hydrometeorological relationship at monthly, seasonal, and annual timescales. Monthly analyses provide the full annual cycle, while seasonal analyses separate the data based on temperature contrasts that influence the fractionation processes. Annual interpretations integrate the longer-term controls, reduce the influence of short-term variability, and provide insights relevant for interpreting paleoclimate archives.

3.1. Variability of precipitation $\delta^{18}O$ and its hydrometeorological controls

Trend analysis of the weekly (non-amount-weighted) precipitation $\delta^{18}O$ record at KPBS revealed a weak but statistically significant long-term enrichment (Sen's slope = +0.071‰ yr^{-1}, Mann-Kendall $p < 0.01$) over the study period (Fig. 3 a). This trend was driven primarily by the warm season (Fig. 3 b), whereas no significant long-term trend was detected during the cold season. $\delta^{18}O$ exhibited a wide distribution of values across cold and warm seasons. In the cold season, $\delta^{18}O$ had a mean of −10.9‰ with values ranging from −27.3 to 0.6‰ (Fig. 4a). The warm season $\delta^{18}O$ showed a mean of −4.6‰ with a minimum of −19‰ to a maximum of 8.4‰. While the ranges were broadly similar, the cold season exhibited greater $\delta^{18}O$ variability with a higher standard deviation (6.0‰) than the warm season (3.5‰). The amount-weighted mean $\delta^{18}O$ (−5.54‰) at KPBS was higher than reported from other mid-western sites, −6.6‰ at Zionsville, Indiana (Tian et al., 2018a) and −6.6‰ at Dayton, Ohio (Bedaso and Wu, 2020). The long-term monthly weighted Local Meteoric Water Line (LMWL) shows a lower slope (6.81 ± 0.21) and intercept (1.68 ± 1.17) in the warm season compared to that in the cold season (7.65 ± 0.19 slope, 3.16 ± 2.49 intercept) (Fig. 4b).

The monthly precipitation amount-weighted $\delta^{18}O$ chronologies were significantly correlated with local hydrometeorological variables, with the strongest relationships observed for temperature ($r = 0.67$) and convective precipitation fraction ($r = 0.65$) (Fig. 5a). The annual average of the amount-weighted monthly $\delta^{18}O$ values ($\delta^{18}O_{annual}$) showed its strongest correlation with convective precipitation rate ($r = 0.56$), followed by VPD ($r = 0.46$) (Fig. 5b). d-excess exhibited a stronger negative correlation ($r = -0.55$) with $\delta^{18}O$ at the annual scale compared to the monthly timescale ($r = -0.25$). Unlike the classic "amount effect" (Dansgaard, 1964) common in coastal CONUS stations (Sun et al., 2019) and many tropical sites – where precipitation $\delta^{18}O$ is negatively correlated with precipitation amount – we observed a positive $\delta^{18}O$-precipitation relationship at the monthly scale (Fig. 5a).

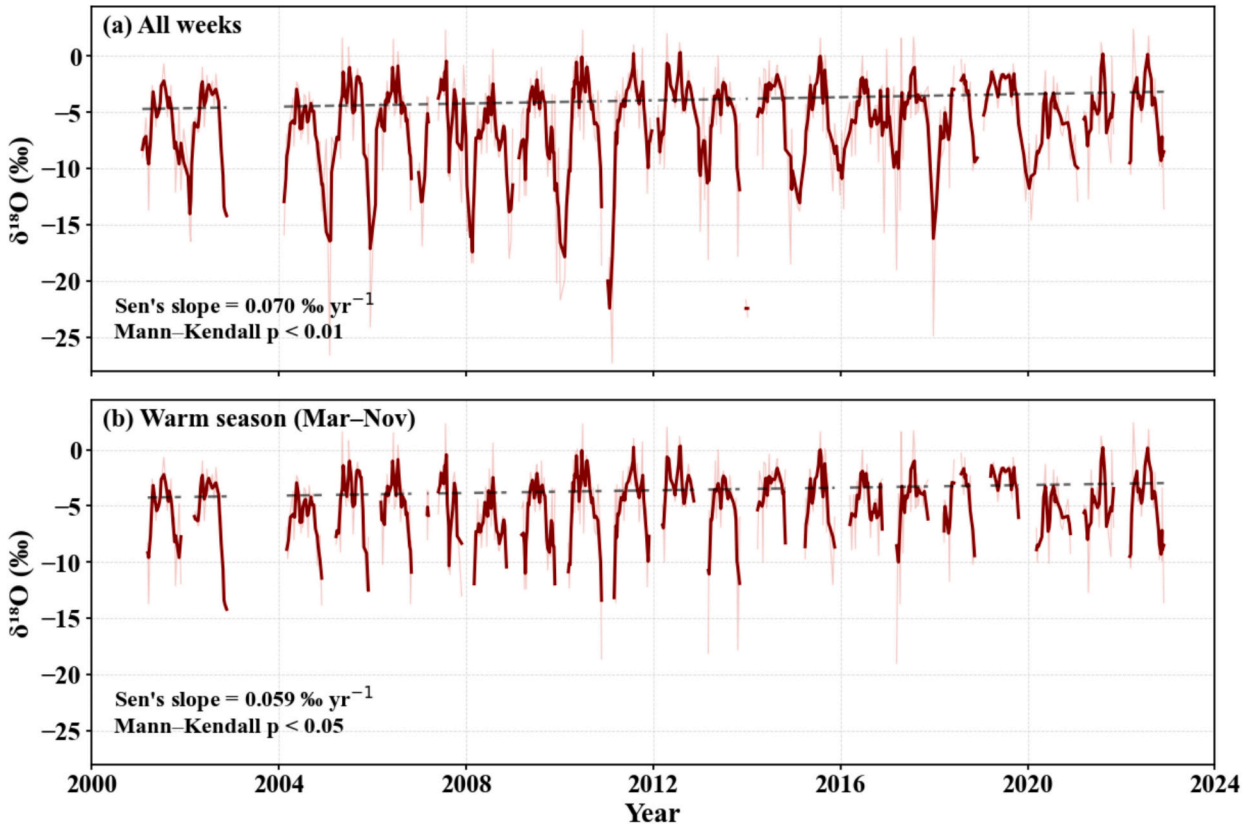

Fig. 3. Weekly precipitation $\delta^{18}O$ timeseries at KPBS from 2001 to 2022 showing (a) the full record and (b) the warm-season subset (March–November). Light lines represent the raw weekly measurements, and dark lines show a 3-week centered running mean to highlight short-term variability. Dashed lines indicate Sen's slope trend. Lines are broken across sampling gaps (>45 days) to avoid implying temporal continuity.

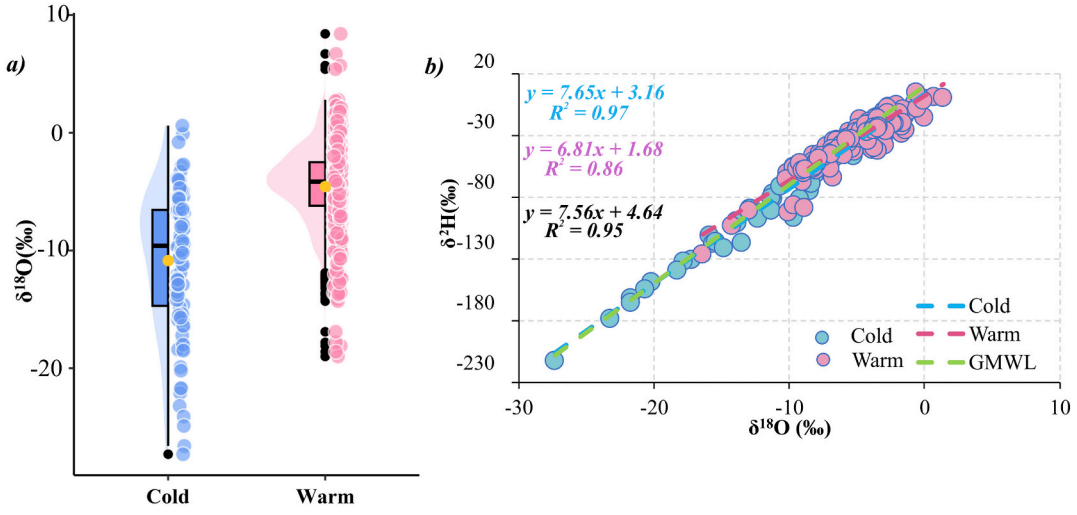

Fig. 4. a) Rain plot showing the distribution of $\delta^{18}O$ during warm- (March–November; pink) and cold (December–February; blue) seasons. b) monthly precipitation amounts with the weighted LMWL for the cold (blue) and warm (pink) seasons. The linear equation shown in black shows the overall LMWL for the KPBS.

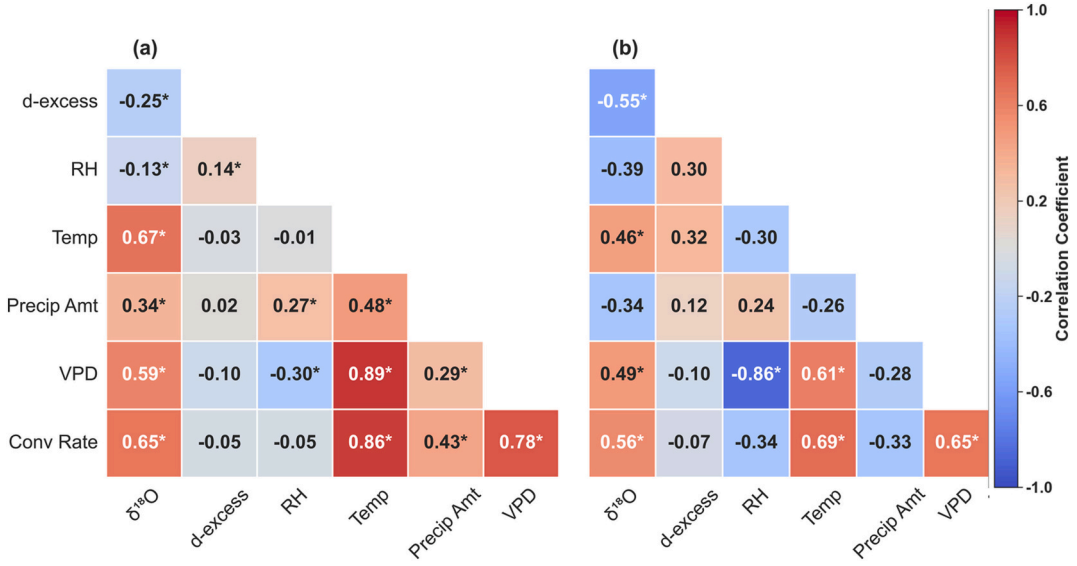

Fig. 5. Heatmap of Pearson correlation coefficients between hydrometeorological parameters and isotopic variables ($\delta^{18}O$ and d-excess) for a) the full time series of individual monthly amount-weighted data and b) annual amount-weighted data. The color scale represents correlation coefficients (−1 to 1), with red indicating positive and blue indicating negative correlations. Asterisks (*) denote statistically significant correlations ($p < 0.05$).

3.2. K-means cluster analysis

The winter season at Konza Prairie was characterized by freezing temperatures and lower VPD, suppressing sub-cloud evaporation. This was evident in the lack of significant correlations between $\delta^{18}O$ and local meteorology and the lack of negative correlations between d-excess and temperature (Table. S1). Despite an overall significant negative relationship between $\delta^{18}O$ and d-excess (Fig. S1), the relationship during the cold season exhibited greater variability and a weaker correlation compared to the warm season, as reflected in the broader distribution of values and lower R^2. Grouping these data using K-means clustering revealed an otherwise hidden pattern in the third cluster. While the rest of the data show negative correlations between d-excess and $\delta^{18}O$, cluster 3 which was mostly comprised of cold season observations (and the 1-2 months preceding or following the cold season) showed a strong positive correlation ($r = 0.62$, p value ≤ 0.001, $n = 65$) (Fig. 6).

3.3. Quantifying moisture source contributions

Overall, the continental sources of moisture contributed most to the precipitation occurring at KPBS compared to the Maritime source (Gulf of Mexico). The temporal evolution of regional moisture source contributions and precipitation isotopes are shown in Fig. 7. Monthly $\delta^{18}O$ variability generally coincided with changes in moisture sources. The moisture originating from the Eastern USA (relatively wet and vegetated) contributed the most, followed by the Western region (relatively dry and vegetated; Fig. S2). The monthly moisture contributions from the Gulf of Mexico showed a significant positive relation to precipitation $\delta^{18}O$ ($r = 0.33$, p value ≤ 0.001) while those from the East and the Great Lakes exhibited a negative relation ($r = -0.22$, p value ≤ 0.01) (Table. 1). Source contributions showed no significant correlation with isotopic variables during the warm season, while the cold season Gulf of Mexico contributions were positively correlated ($r = 0.35$, P value ≤ 0.05) with $\delta^{18}O$. While monthly moisture contributions significantly correlate with the isotopic data, no such relationship is evident at the annual scale.

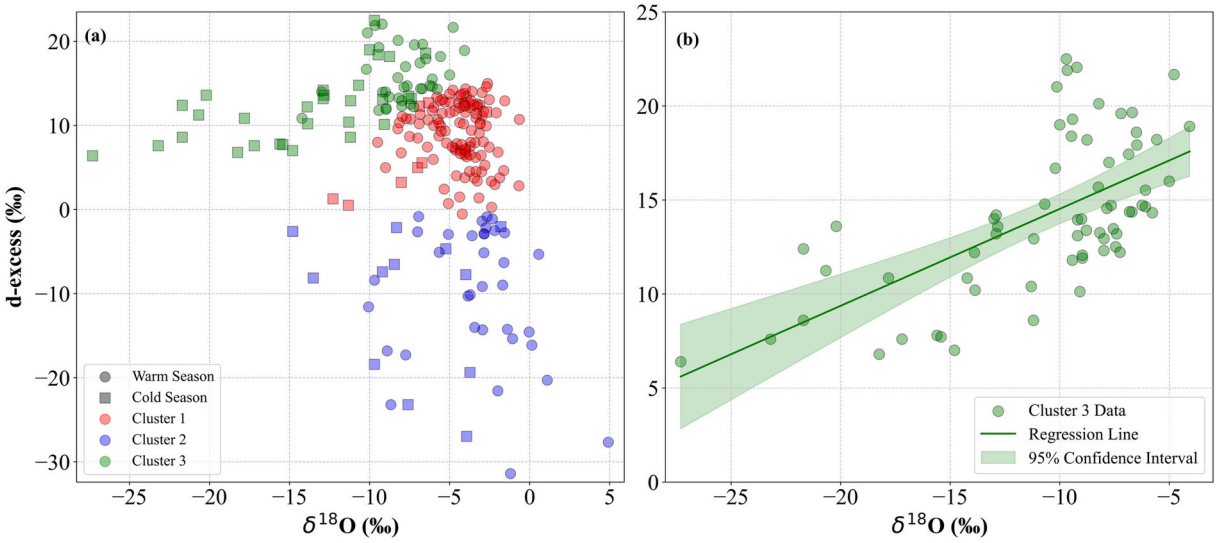

Fig. 6. a) The $\delta^{18}O$-d-excess diagram showing the cold and warm season variability with distinct clustering patterns, and b) Linear regression analysis for cluster 3, illustrating a significant positive correlation with a 95% confidence interval in the shaded region.

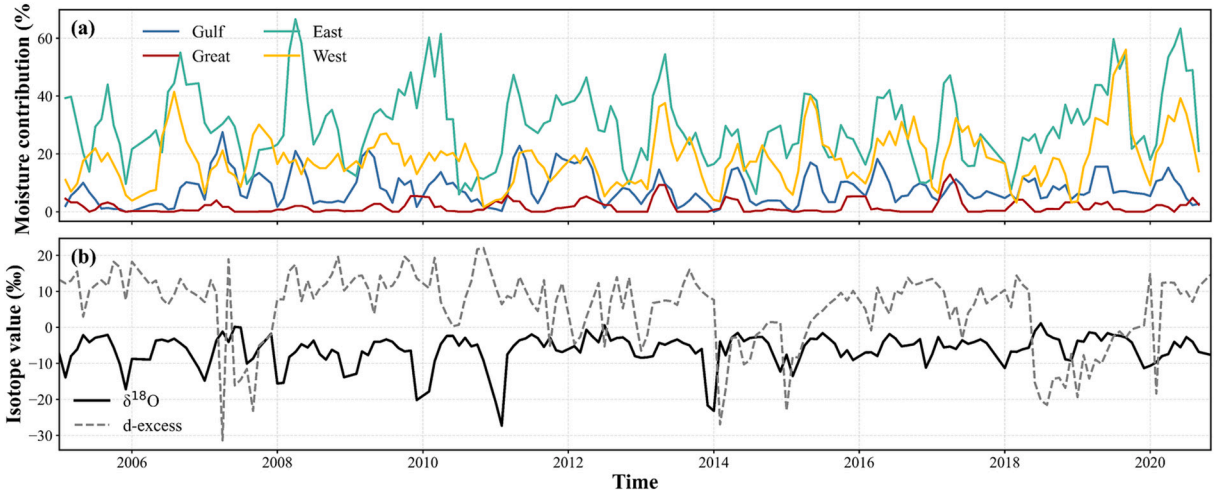

Fig. 7. Time series comparisons of regional moisture source contributions and precipitation isotope variables. A) monthly regional moisture contributions from the Gulf of Mexico (Gulf), the Great Lakes (Great), the Eastern continental region (East), and the Western continental region (West). Monthly precipitation isotope values showing $\delta^{18}O$ (solid line), and d-excess (dashed line) along with regional moisture contributions (dimensionless) calculated from the summed fractional moisture uptake within each source region.

Table 1
The correlations between $\delta^{18}O$ and moisture contributions from various sources at the monthly scale and cold seasons. No significant correlations were observed during the warm season.

Source	Data type	Variable	r	*P value*
Gulf	Monthly	$\delta^{18}O$	0.33	5.61×10^{-6}
Great Lakes			−0.22	0.003
East			−0.22	0.003
North/Polar			−0.16	0.04
Gulf	Cold season	$\delta^{18}O$	0.35	0.03

However, excluding the record-breaking drought year of 2012 (Hoerling et al., 2014), annual moisture contributions from the western and eastern CONUS exhibited opposing correlations with $\delta^{18}O$: negative for contributions from Eastern CONUS ($r = 0.76$, p value ≤ 0.01) and positive for Western CONUS ($r = 0.72$, p value ≤ 0.01). These findings suggest that the 2012 $\delta^{18}O$ signature was strongly influenced by local meteorological conditions, as indicated by the highest VPD recorded during the study period.

4. Discussion

4.1. *Influence of local hydrometeorology on $\delta^{18}O$*

Monthly amount weighted precipitation $\delta^{18}O$ at KPBS is primarily governed by warm-season atmospheric dynamics, particularly convective activity and associated thermodynamic conditions. Overall, the results indicate that $\delta^{18}O$ variability reflects seasonal coupling between temperature, VPD, and convective fraction of precipitation. At the monthly scale, $\delta^{18}O$ shows moderate to strong positive correlations with temperature ($r = 0.67$), VPD ($r = 0.59$), and convective rate ($r = 0.65$), whereas the correlation with precipitation amount is weaker ($r = 0.34$). These relationships suggest that isotopic enrichment at KPBS is closely linked to warm-season convection and atmospheric drying. Temperature, VPD, and convective activity are strongly intercorrelated ($r = 0.89$ between temperature and VPD; $r = 0.86$ between temperature and

convective rate.; $r = 0.78$ between VPD and convective rate; Fig. 5a), indicating $\delta^{18}O$ that variability reflects integrated seasonal atmospheric conditions. The positive relationship between $\delta^{18}O$ and precipitation amount at the monthly scale, therefore, likely reflects seasonal covariance, whereby both precipitation and isotopic enrichment peak during the summer (Sun et al., 2019). Such seasonality has been documented in other mid-latitude continental regions, where apparent deviations from the classic "amount effect" arise from temperature- and convection-driven controls rather than event-scale rainout (Bedaso and Wu, 2020; Tian et al., 2018a).

Convective precipitation accounts for 30–70% (Andresen et al., 2012) of warm-season precipitation in the Midwest and about 73% for KPBS over the sampling period. Convective precipitation shows a strong positive correlation with $\delta^{18}O$. Following the mechanism proposed by Aggarwal et al. (2016), ice particles in convective systems grow rapidly through accretion as they are lofted by strong updrafts, during which supercooled boundary-layer water freezes onto the surface of the condensation nuclei. As a result, rainout from the convective clouds retains an isotopic composition that closely reflects that of the boundary layer (Sun et al., 2019). Under these conditions, $\delta^{18}O$ reflects the intensity and location of convective activity (or the moisture sourcing), rather than local precipitation amount. The weakening of the positive relationship between $\delta^{18}O$ and precipitation amount at the annual scale, with decreased correlations between $\delta^{18}O$ and convective rate (Fig. 5 b), supports that the monthly data are dominated by seasonal effects. This interpretation is consistent with findings from monsoon-dominated regions, where precipitation $\delta^{18}O$ often exhibits spatially coherent patterns linked to large-scale atmospheric circulation despite varied local precipitation distributions (Duan et al., 2023; Kathayat et al., 2022). In eastern China, for example, summer precipitation may display dipole or tripole rainfall structures, whereas $\delta^{18}O_P$ reflects broader circulation-driven signals (Duan et al., 2023). A similar mechanism may operate at KPBS, where the location and strength of upstream convection associated with the GPLLJ modulate the isotopic composition of precipitation. The weakening of the $\delta^{18}O$–precipitation relationship at the annual scale further supports that seasonal and circulation-driven dynamics dominate the monthly signal. The stronger negative correlation between d-excess and $\delta^{18}O$ at annual timescales when compared to monthly timescales was consistent with enhanced kinetic effects associated with sub-cloud evaporation, suggesting an enhanced role of local hydrometeorology in the $\delta^{18}O_{annual}$ (Xia and Winnick, 2021).

Similar to the "inverse amount effect" (positive correlation between rainfall amount and precipitation $\delta^{18}O$) observed at KPBS, this pattern has also been documented at another midwestern CONUS site, Zionsville, Indiana (Tian et al., 2018b) and in certain tropical sites in southern India (Lekshmy et al., 2015; Yadava et al., 2007). The strong positive relationship between $\delta^{18}O$ and the convective fraction on both monthly and annual timescales indicates that the inverse amount effect may arise from the dominance of convective precipitation that accounts for 30–70% of warm-season precipitation (Andresen et al., 2012). The enriched isotopic signatures of convective precipitation (Aggarwal et al., 2016) can mask the depleted isotopic signals associated with non-convective events, particularly during the warm season when nearly 75% of the annual precipitation occurs. The shift from the significant "inverse amount effect" at the monthly scale to a non-significant amount effect at the annual scale, along with a weaker correlation between $\delta^{18}O$ and convective fraction, is consistent with this pattern.

In contrast to this interpretation, the tenet that isotope ratios reflect rain-type (convective or stratiform) proportions (Aggarwal et al., 2016) was recently challenged by Yu et al. (2024). Yu et al. (2024) argued that $\delta^{18}O$ also remains strongly correlated to convection intensity but independent of rain-type proportions because stratiform precipitation isotope ratios span a wide range of values. Although the Yu et al., 2024 interpretation was supported using data from pantropical sites, we explored this perspective because the correlation of $\delta^{18}O$-convective fraction applies to non-tropical sites as well (Sun et al., 2019). Our data illustrate higher stratiform fractions (lower convective fractions) cover a large range of isotopic values. However, contrary to what was observed by Yu et al. (2024), correlation with the convective strength (lower outgoing longwave radiation- more cloud cover) was lower ($r = 0.54$) compared to that of convective rate ($r = 0.65$) (not shown here).

4.2. Below-cloud evaporation and the anomalously low d-excess values

Fig. 6 reveals two contrasting $\delta^{18}O$-d-excess patterns reflecting seasonal differences in the dominant fractionation processes affecting precipitation isotopes at KPBS. Because d-excess reflects the differential fractionation of hydrogen and oxygen isotopes and is particularly sensitive to kinetic processes such as sub-cloud evaporation (Craig et al., 1963), variability in d-excess provides insights into evaporative modification of precipitation. Although d-excess is mathematically defined as $\delta^{2}H\text{-}8\times\delta^{18}O$, a systematic relationship with $\delta^{18}O$ emerges only when its variability relative to $\delta^{18}O$ primarily reflects kinetic modifications rather than a mathematical relationship.

Most of the samples, particularly during the warm season, show a negative $\delta^{18}O$-d-excess relationship. This pattern is consistent with Rayleigh distillation and kinetic fractionation associated with below-cloud raindrop evaporation under unsaturated conditions (Craig et al., 1963; Landais et al., 2010; Laskar et al., 2014; Sun et al., 2024; Tian et al., 2018a; Xia and Winnick, 2021). Enhanced warm-season convective activity can transport recycled continental moisture, while seasonally higher VPD favors kinetic fractionation during raindrop descent, enriching $\delta^{18}O$ and reducing d-excess values. When such convection occurs under higher relative humidity conditions, the entrained moisture will reflect the isotopic composition similar to the surface water/soil moisture. The increased correlation between d-excess and VPD during the warm season (Table S1) further supports this interpretation and is consistent with the low d-excess values observed in Great Plains surface waters (Bowen et al., 2007).

In contrast, cluster 3 represents a distinct cold-season isotopic pattern characterized by higher d-excess with a statistically significant positive correlation between d-excess and $\delta^{18}O$ (Fig. 6 b). This behavior is inconsistent with below-cloud evaporation and instead reflects a greater in-cloud fractionation process and large-scale dynamics. During the cold season, regional vegetation is dormant and/or senesced, and potential evapotranspiration is low, limiting the contribution of recycled moisture to local precipitation (Singer et al., 2021). Under these cold-season hydrometeorological conditions, isotopic signatures are generally less affected by below-cloud evaporation and more strongly influenced by colder, high-latitude moisture sources (Bedaso and Wu, 2020) and kinetic fractionation associated with supersaturation during cloud formation, thus increasing d-excess (Deshpande et al., 2013; Graf et al., 2019; Merlivat and Jouzel, 1979).

These contrasting seasonal behaviors highlight that warm-season precipitation is associated with reduced d-excess owing to evaporation and convective processes. In contrast, cold-season precipitation exhibits enhanced d-excess driven by in-cloud supersaturation and large-scale moisture transport. While cluster 3 comprises only a small fraction of the overall dataset, it is a useful subset for isolating processes that are otherwise masked by evaporation-led isotopic effects. These results highlight that the application of d-excess as a paleo-meteoric tracer requires careful consideration of seasonality and synoptic/thermodynamic conditions.

4.3. d-excess variability and isotopic similarity during extreme wet and dry years

Based on the annual isotopic composition of precipitation at KPBS, years with distinct isotopic values were identified and the potential causes were investigated. The high $\delta^{18}O_{Ann}$ values (−3.7‰ in 2012 and − 3.6‰ in 2019) accompanied by low d-excess values (4.9‰ in 2012 and − 6.7‰ in 2019) during two contrasting hydroclimatic years,

extremely dry (2012- lowest precipitation and highest VPD during the study period, 565.9 mm and 0.87 kPa respectively) and wet (2019- above average precipitation- 1142 mm and relatively humid atmospheric conditions) (Fig. 8 a), presented an unexpected pattern. Despite contrasting hydroclimatic extremes (i.e., dry vs. wet), these years showed comparable isotopic patterns, indicating that different atmospheric pathways can still result in similar isotopic behavior. This equifinality underscores the complexity of interpreting precipitation isotope records, as similar $\delta^{18}O$ and d-excess patterns may arise from fundamentally different combinations of atmospheric aridity, moisture sourcing, and circulation dynamics.

The higher $\delta^{18}O_{Ann}$ in 2012 coincides with the highest VPD observed during the study period, suggesting a dominant influence of local meteorological conditions that likely overprinted the isotopic signal of distal moisture sources. In terms of the annual moisture uptake pattern, 2012 exhibited the lowest overall contributions from continental sources, whereas 2019 showed enhanced uptake from continental sources. Hoerling et al., 2014 showed that the 2012 drought in the central U.S, was exacerbated by a reduction in the moisture flux from the Gulf of Mexico. However, at KPBS, the annual Gulf of Mexico percentage contribution was above average, likely due to diminished land-atmosphere feedback (Herrera-Estrada et al., 2019). The higher $\delta^{18}O$ in 2012 likely reflects this increased percentage contribution from the Gulf, intense continental evaporation under dry conditions, and increased local aridity. In 2019, although the 500 hPa geopotential height anomalies (Fig. 9) resembled the zonal wave train pattern linked to heavy midwestern precipitation events (Zhang and Villarini, 2019), the trough over the western and central CONUS did not extend to northeast Kansas. However, the ridge over the central US was weak and coincided with strong low-level (850 hPa) moisture transport, resulting

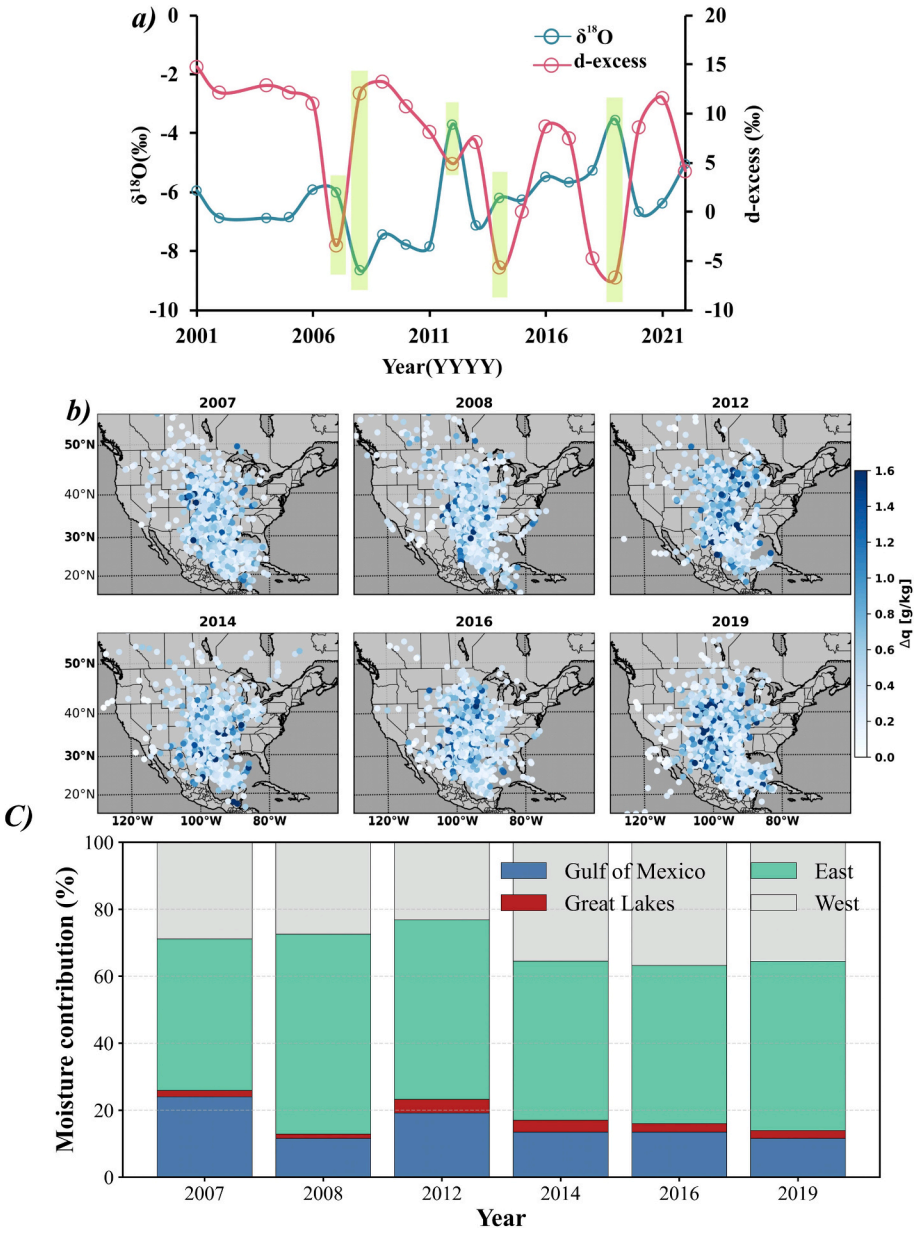

Fig. 8. a) Annual averages of monthly amount weighted $\delta^{18}O$ and d-excess at Konza Prairie. Light green shading highlights years with distinct isotopic signatures in either $\delta^{18}O$ or d-excess. b) Clusters of annual moisture uptake locations during the isotopically distinct years, based on differences in specific humidity between two-time intervals (Δq). c) Interannual variability in regional moisture source contributions to precipitation at Konza Prairie Biological Station (KPBS) for the selected years (2007, 2008, 2012, 2014, 2016, and 2019). Stacked bars show the percentage contribution of moisture originating from the Gulf of Mexico (blue), Great Lakes (red), Eastern CONUS, and Western CONUS.

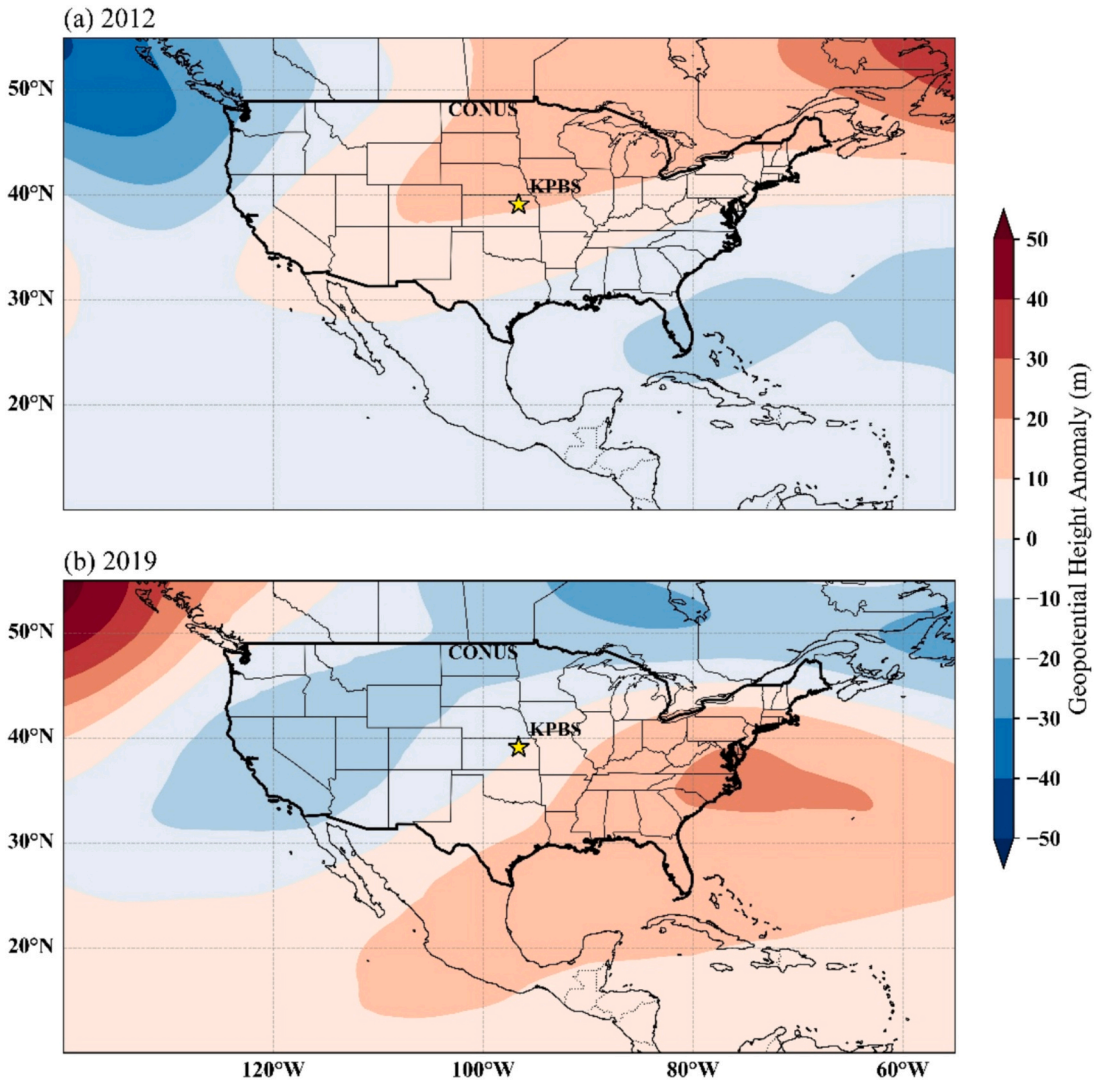

Fig. 9. Spatial distribution of the 500-hPa geopotential anomalies for: a) year 2012 and b) year 2019; during the study season (2001−2022): Positive anomalies (red shades) indicate higher-than average heights, while negative anomalies (blue shades) indicate lower-than-average heights relative to the 2001–2022 climatology. The study location, KPBS, is marked with a star, and the boundary of CONUS is outlined with a thick black border.

in intense precipitation across the region (Fig. S3 b). Gulf of Mexico moisture brought by the GPLLJ converged near Texas, and as suggested by the back trajectories, subsequent moisture uptake occurred from this region and farther north (Fig. 8 b). The resultant convective updraft likely occurred under higher humidity conditions, resulting in reduced kinetic fractionation; thus, the isotopic signatures resembled the evaporative waters of the southern coasts (Bowen et al., 2007) that are mainly fed by the Gulf (high $\delta^{18}O$ and low d-excess). In contrast, strong positive geopotential anomalies across much of the CONUS indicated a dominant mid-tropospheric ridge in 2012. At the same time, the 850 hPa moisture transport and divergence fields revealed a weaker GPLLJ and widespread moisture divergence over Kansas (Fig. S3 a). The extreme drought brought arid conditions to KPBS leading to enriched $\delta^{18}O$ and reduced d-excess via enhanced sub cloud evaporation and associated kinetic fractionation.

Notably, in 2007, the Gulf of Mexico moisture contributions increased (27.9%; highest among the whole study period) with the second lowest continental contributions, resulting in a d-excess (−3.5‰) reflective of the south coast. The years with comparatively higher d-excess have coincided with the contributions from the eastern CONUS (2008, 2011, and 2016) that hold the highest d-excess regions in the CONUS (Bowen et al., 2007). Additionally, it is also noted that the negative precipitation d-excess coincided with fewer differences in moisture contributions between the eastern and western CONUS (Fig. S4) indicating that these anomalously low d-excess values could be attributed to the increased moisture uptake from the west, as was the case for years 2007 and 2014 (Fig. 8).

Quantitative comparison of annual moisture contributions shows that continental sources consistently dominate precipitation at KPBS, with the Eastern CONUS source being the largest contributor. Interannual variability is therefore mostly controlled by shifts in the continental recycling intensity and the atmospheric processes. We note that d-excess variability depends on the combined influence of humidity conditions at the moisture source, Rayleigh fractionation during moisture transport, and local kinetic modification. Isotopic similarity during extreme years results from combinations of boundary-layer evaporation, recycled-moisture entrainment, and large-scale circulation dynamics. Although the moisture contributions from Gulf of Mexico to the KPBS are smaller compared to the continental sources, its influence remains critical in shaping the precipitation patterns across the Great Plains as a whole and to Konza Prairie specifically. As the primary source of moisture flux to the western CONUS, the Gulf's influence on d-excess is substantial, which is mediated by the GPLLJ that acts as a key nexus between the oceanic and terrestrial moisture sources (Sala, 2025).

5. Conclusions and implications

The >20-year precipitation isotope record from KPBS reveals that $\delta^{18}O$ variability is primarily governed by warm-season atmospheric dynamics rather than by the classic precipitation "amount effect." In tropical regions, the traditional amount effect describes a negative relationship between $\delta^{18}O$ and precipitation amount, whereby heavier rainfall is associated with lower $\delta^{18}O$. In contrast, we observe a positive relationship between $\delta^{18}O$ and precipitation amount at the monthly scale, indicating that periods of enhanced precipitation coincide with isotopic enrichment. This "inverse amount effect" reflects seasonal covariance between precipitation, temperature, VPD, and convective activity, all of which peak during the warm season. At the annual scale, this relationship weakens, consistent with the integration of multiple seasonal processes.

During the cold season, precipitation $\delta^{18}O$ is less influenced by local thermodynamic conditions and more strongly controlled by in-cloud fractionation processes and large-scale moisture transport from the Gulf of Mexico and the eastern CONUS. These seasonal contrasts demonstrate that $\delta^{18}O$ at this continental interior site reflects the combined influence of convective regime, upstream moisture sourcing, and sub-cloud evaporation rather than local precipitation amount alone.

Our results further show that warm-season $\delta^{18}O$ is closely linked to atmospheric aridity, as shown by persistent correlations with VPD and enhanced evaporative modification during dry conditions. Extreme years highlight this coupling: elevated $\delta^{18}O$ values during the 2012 drought and 2019 wet year reflect differing combinations of atmospheric dryness and moisture source variability. These findings underscore the importance of both below-cloud evaporation large-scale circulation dynamics, including transport via the Great Plains low-level jet, in defining precipitation isotope signal.

These results have important implications for interpreting ecohydrological proxies. Because precipitation $\delta^{18}O$ integrates both local evaporative demand and remote moisture transport processes, hydroclimate reconstructions in temperate continental interiors must account for seasonal dynamics, atmospheric aridity, and circulation variability. As climate change is projected to alter both humidity regimes and oceanic moisture transport pathways, improved understanding of these competing controls will be critical for evaluating isotope-enabled climate model simulations and future hydroclimate projections.

CRediT authorship contribution statement

Saranya Puthalath: Writing – original draft, Methodology, Investigation, Formal analysis, Data curation, Conceptualization. **Matthew F. Kirk:** Writing – review & editing. **Rachel M. Keen:** Writing – review & editing, Data curation. **Alejandro N. Flores:** Writing – review & editing. **Sharon A. Billings:** Writing – review & editing. **Pamela L. Sullivan:** Writing – review & editing. **Jesse B. Nippert:** Writing – review & editing, Supervision, Resources, Funding acquisition.

Declaration of competing interest

The authors declare that they have no known competing financial interests or personal relationships that could have appeared to influence the work reported in this paper.

Acknowledgements

We acknowledge funding support from the Konza Prairie LTER (NSF LTER 1440484, 2415980, 2121652, 2121694, 2121639, and 2121595) program. We are grateful to Prof. Hoori Ajami (University of California, Riverside), Prof. Daniel Hirmas (Texas Tech University), Prof. Kamini Singha (Colorado School of Mines), and Prof. Li Li (Penn State) for discussions and valuable comments on this manuscript. We also thank the four anonymous reviewers for their constructive comments and suggestions, which helped improve the clarity and quality of this manuscript.

Appendix A. Supplementary data

Supplementary data to this article can be found online at https://doi.org/10.1016/j.scitotenv.2026.181790.

Data availability

Data records from the Konza Prairie Biological Station are publicly available in the Environmental Data Initiative (EDI) data portal and are cited in the methods.

References

Adhikari, N., Gao, J., Yao, T., Yang, Y., Dai, D., 2020. The main controls of the precipitation stable isotopes at Kathmandu, Nepal. Tellus Ser. B Chem. Phys. Meteorol. 72, 1–17. https://doi.org/10.1080/16000889.2020.1721967.

Aggarwal, P.K., Romatschke, U., Araguas-Araguas, L., Belachew, D., Longstaffe, F.J., Berg, P., Schumacher, C., Funk, A., 2016. Proportions of convective and stratiform precipitation revealed in water isotope ratios. Nat. Geosci. 9, 624–629. https://doi.org/10.1038/ngeo2739.

Andresen, Jeff, Hilberg, S., Kunkel, K., Winkler, J., Andresen, J., Hatfield, J., Bidwell, D., Brown, D., 2012. Historical climate and climate trends in the midwestern USA national climate assessment midwest technical input report. In: US Natl. Clim. Assess. (Midwest Tech. Input Rep. 1–18.).

Bedaso, Z., Wu, S.Y., 2020. Daily precipitation isotope variation in Midwestern United States: implication for hydroclimate and moisture source. Sci. Total Environ. 713, 1–13. https://doi.org/10.1016/j.scitotenv.2020.136631.

Blair, J.M., 2023. Weekly, seasonal and annual measurement of precipitation volume and chemistry collected as part of the National Atmospheric Deposition Program at Konza Prairie [WWW Document]. Environ. Data Initiat. https://doi.org/10.6073/pasta/295644787ee8a1c00edd6f48dde75c4e.

Bonner, W.D., 1968. Climatology of the Low Level Jet. Mon. Weather Rev. 96, 833–850. https://doi.org/10.1175/1520-0493(1968)096<0833:cotllj>2.0.co;2.

Bowen, G.J., Ehleringer, J.R., Chesson, L.A., Stange, E., Cerling, T.E., 2007. Stable isotope ratios of tap water in the contiguous United States. Water Resour. Res. 43, 1–12. https://doi.org/10.1029/2006WR005186.

Broz, A., Retallack, G.J., Maxwell, T.M., et al., 2021. A record of vapour pressure deficit preserved in wood and soil across biomes. Sci. Rep. 11, 662. https://doi.org/10.1038/s41598-020-80006-9.

Craig, H., Gordon, L., Horibe, Y., 1963. Isotopic exchange effects in the evaporation of water. J. Geophys. Res. 68, 5079–5087.

Dansgaard, W., 1964. Stable isotopes in precipitation. Tellus 16, 436–468. https://doi.org/10.3402/tellusa.v16i4.8993.

Deangelis, A., Dominguez, F., Fan, Y., Robock, A., Kustu, M.D., Robinson, D., 2010. Evidence of enhanced precipitation due to irrigation over the Great Plains of the United States. J. Geophys. Res. Atmos. 115, 1–14. https://doi.org/10.1029/2010JD013892.

Deng, Y., Li, X., Shi, F., Hu, X., 2021. Woody plant encroachment enhanced global vegetation greening and ecosystem water-use efficiency. Glob. Ecol. Biogeogr. 30, 2337–2353. https://doi.org/10.1111/geb.13386.

Deshpande, R.D., Maurya, A.S., Kumar, B., Sarkar, A., Gupta, S.K., 2013. Kinetic fractionation of water isotopes during liquid condensation under super-saturated condition. Geochim. Cosmochim. Acta 100, 60–72. https://doi.org/10.1016/j.gca.2012.10.009.

Draxler, R.R., Hess, G.D., 1998. An overview of the HYSPLIT_4 modelling system for trajectories, dispersion and deposition. Aust. Meteorol. Mag. 47, 295–308.

Duan, P., Li, H., Ma, Z., Zhao, J., Dong, X., Sinha, A., Hu, P., Zhang, H., Cai, Y., Ning, Y., Edwards, R.L., Cheng, H., 2023. Interdecadal to centennial climate variability surrounding the 8.2 ka event in North China revealed through an annually resolved speleothem record from Beijing. Geophys. Res. Lett. 50, 1–11. https://doi.org/10.1029/2022GL101182.

Ficklin, D.L., Novick, K.A., 2017. Historic and projected changes in vapor pressure deficit suggest a continental-scale drying of the United States atmosphere. J. Geophys. Res. 122, 2061–2079. https://doi.org/10.1002/2016JD025855.

Graf, P., Wernli, H., Pfahl, S., Sodemann, H., 2019. A new interpretative framework for below-cloud effects on stable water isotopes in vapour and rain. Atmos. Chem. Phys. 19, 747–765. https://doi.org/10.5194/acp-19-747-2019.

Herrera-Estrada, J.E., Martinez, J.A., Dominguez, F., Findell, K.L., Wood, E.F., Sheffield, J., 2019. Reduced moisture transport linked to drought propagation across North America. Geophys. Res. Lett. 46, 5243–5253. https://doi.org/10.1029/2019GL082475.

Hoerling, M., Eischeid, J., Kumar, A., Leung, R., Mariotti, A., Mo, K., Schubert, S., Seager, R., 2014. Causes and predictability of the 2012 great plains drought. Bull. Am. Meteorol. Soc. 95, 269–282. https://doi.org/10.1175/BAMS-D-13-00055.1.

Jasechko, S., Sharp, Z.D., Gibson, J.J., Birks, S.J., Yi, Y., Fawcett, P.J., 2013. Terrestrial water fluxes dominated by transpiration. Nature 496, 347–350. https://doi.org/10.1038/nature11983.

Jouzel, J., Merlivat, L., 1984. Deuterium and oxygen 18 in precipitation: modeling of the isotopic effects during snow formation. J. Geophys. Res. 89 (D7), 11749–11757. https://doi.org/10.1029/JD089iD07p11749.

Kanungo, T., Mount, D.M., Netanyahu, N.S., Piatko, C.D., Silverman, R., Wu, A.Y., 2002. An efficient k-means clustering algorithms: Analysis and implementation. IEEE Trans. Pattern Anal. Mach. Intell. 24, 881–892. https://doi.org/10.1109/TPAMI.2002.1017616.

Kathayat, G., Sinha, A., Breitenbach, S.F.M., Tan, L., Spötl, C., Li, H., Dong, X., Zhang, H., Ning, Y., Allan, R.J., Damodaran, V., Edwards, R.L., Cheng, H., 2022. Protracted Indian monsoon droughts of the past millennium and their societal impacts. Proc. Natl. Acad. Sci. USA 119. https://doi.org/10.1073/pnas.2207487119.

Keen, R.M., Sadayappan, K., Jarecke, K.M., Li, L., Kirk, M.F., Sullivan, P.L., Nippert, J.B., 2024. Unexpected hydrologic response to ecosystem state change in tallgrass prairie. J. Hydrol. 643. https://doi.org/10.1016/j.jhydrol.2024.131937.

Knapp, A.K., Chen, A., Griffin-Nolan, R.J., Baur, L.E., Carroll, C.J.W., Gray, J.E., Hoffman, A.M., Li, X., Post, A.K., Slette, I.J., Collins, S.L., Luo, Y., Smith, M.D., 2020. Resolving the dust bowl paradox of grassland responses to extreme drought. Proc. Natl. Acad. Sci. USA 117, 22249–22255. https://doi.org/10.1073/pnas.1922030117.

Landais, A., Risi, C., Bony, S., Vimeux, F., Descroix, L., Falourd, S., Bouygues, A., 2010. Combined measurements of 17 O excess and d-excess in African monsoon precipitation : Implications for evaluating convective parameterizations. Earth Planet. Sci. Lett. 298, 104–112. https://doi.org/10.1016/j.epsl.2010.07.033.

Laskar, A.H., Huang, J.C., Hsu, S.C., Bhattacharya, S.K., Wang, C.H., Liang, M.C., 2014. Stable isotopic composition of near surface atmospheric water vapor and rain-vapor interaction in Taipei, Taiwan. J. Hydrol. 519, 2091–2100. https://doi.org/10.1016/j.jhydrol.2014.10.017.

Lekshmy, P.R., Midhun, M., Ramesh, R., Jani, R.A., 2014. 18 O depletion in monsoon rain relates to large scale organized convection rather than the amount of rainfall. Sci. Rep. 4. https://doi.org/10.1038/srep05661.

Lekshmy, P.R., Midhun, M., Ramesh, R., 2015. Spatial Variation of Amount Effect Over Peninsular India and Sri Lanka: Role of Seasonality 5500–5507. https://doi.org/10.1002/2015GL064517. Received.

Merlivat, L., Jouzel, J., 1979. Global climatic interpretation of the deuterium-oxygen 16 relationship for precipitation. J. Geophys. Res. 84, 5029–5033. https://doi.org/10.1029/JC084iC08p05029.

Miller, J.A., Appel, C.L., 1997. Ground Water Atlas of the United States; Kansas, Missouri, and Nebraska, 24. U.S. Geol. Surv. Hydrologic.

Molina, M.J., Allen, J.T., Prein, A.F., 2020. Moisture attribution and sensitivity analysis of a winter Tornado outbreak. Weather Forecast. 35, 1263–1288. https://doi.org/10.1175/WAF-D-19-0240.1.

Nippert, J.B., Ahlering, M.A., Fuhlendorf, S.D., Helzer, C.J., McMillan, N.A., Ratajczak, Z., 2026. Rethinking grassland management in the Great Plains during the era of woody plant encroachment. BioScience, biag033. https://doi.org/10.1093/biosci/biag033.

Pfahl, S., Madonna, E., Boettcher, M., Joos, H., Wernli, H., 2014. Warm conveyor belts in the ERA-Interim Dataset (1979-2010). Part II: moisture origin and relevance for precipitation. J. Clim. 27, 27–40. https://doi.org/10.1175/JCLI-D-13-00223.1.

Rahul, P., Ghosh, P., 2018. Long term observations on stable isotope ratios in rainwater samples from twin stations over Southern India; identifying the role of amount effect, moisture source and rainout during the dual monsoons. Clim. Dyn. 0 (0). https://doi.org/10.1007/s00382-018-4552-1.

Ratajczak, Z., Nippert, J.B., Collins, S.L., 2012. Woody encroachment decreases diversity across North American grasslands and savannas. Ecology 93, 697–703. https://doi.org/10.1890/11-1199.1.

Rozanski, K., Araguás-Araguás, L., Gonfiantini, R., 1993. Isotopic patterns in modern global precipitation. In: Climate Change in Continental Isotopic Records, Geophysical. Monograph. Series, pp. 1–36. https://doi.org/10.1029/gm078p0001.

Sadayappan, K., Keen, R., Jarecke, K.M., Moreno, V., Nippert, J.B., Kirk, M.F., Sullivan, P.L., Li, L., 2023. Drier streams despite a wetter climate in woody-encroached grasslands. J. Hydrol. 627. https://doi.org/10.1016/j.jhydrol.2023.130388.

Sala, C.M., 2025. Ocean and land moisture contributions to Midwest United States summertime precipitation. Clim. Dyn. 63. https://doi.org/10.1007/s00382-025-07617-8.

Salati, E., Dall'Olio, A., Matsui, E., Gat, J.R., 1979. Recycling of water in the Amazon Basin: an isotopic study. Water Resour. Res. 15, 1250–1258. https://doi.org/10.1029/WR015i005p01250.

Saranya, P., Krishan, G., Rao, M.S., Kumar, S., Kumar, B., 2018a. Controls on water vapor isotopes over Roorkee, India: impact of convective activities and depression systems. J. Hydrol. 557, 679–687. https://doi.org/10.1016/j.jhydrol.2017.12.061.

Saranya, P., Krishan, G., Rao, M.S., Kumar, S., Kumar, B., 2018b. Controls on water vapor isotopes over Roorkee, India: impact of convective activities and depression systems. J. Hydrol. 557, 679–687. https://doi.org/10.1016/j.jhydrol.2017.12.061.

Saranya, P., Krishnakumar, A., Sinha, N., Kumar, S., Anoop Krishnan, K., 2021. Isotopic signatures of moisture recycling and evaporation processes along the Western Ghats orography. Atmos. Res. 264. https://doi.org/10.1016/j.atmosres.2021.105863.

Simpson, I.R., McKinnon, K.A., Kennedy, D., Lawrence, D.M., Lehner, F., Seager, R., 2024. Observed humidity trends in dry regions contradict climate models. Proc. Natl. Acad. Sci. USA 121, 1–12. https://doi.org/10.1073/pnas.2302480120.

Singer, M.B., Asfaw, D.T., Rosolem, R., Cuthbert, M.O., Miralles, D.G., MacLeod, D., Quichimbo, E.A., Michaelides, K., 2021. Hourly potential evapotranspiration at 0.1° resolution for the global land surface from 1981-present. Sci. Data 8, 1–13. https://doi.org/10.1038/s41597-021-01003-9.

Sodemann, H., 2025. The Lagrangian moisture source and transport diagnostic WaterSip V3.2. Geosci. Model Dev. 18, 8887–8926. https://doi.org/10.5194/gmd-18-8887-2025.

Sodemann, H., Masson-Delmotte, V., Schwierz, C., Vinther, B.M., Wernli, H., 2008. Interannual variability of Greenland winter precipitation sources: 2. Effects of North Atlantic Oscillation variability on stable isotopes in precipitation. J. Geophys. Res. Atmos. 113. https://doi.org/10.1029/2007JD009416.

Stein, A.F., Draxler, R.R., Rolph, G.D., Stunder, B.J.B., Cohen, M.D., Ngan, F., 2015. Noaa's hysplit atmospheric transport and dispersion modeling system. Bull. Am. Meteorol. Soc. 96, 2059–2077. https://doi.org/10.1175/BAMS-D-14-00110.1.

Stevens, N., Lehmann, C.E.R., Murphy, B.P., Durigan, G., 2017. Savanna woody encroachment is widespread across three continents. Glob. Chang. Biol. 23, 235–244. https://doi.org/10.1111/gcb.13409.

Sun, C., Shanahan, T.M., Partin, J., 2019. Controls on the isotopic composition of precipitation in the south-central United States. J. Geophys. Res. Atmos. 124, 8320–8335. https://doi.org/10.1029/2018JD029306.

Sun, C., Shanahan, T., He, S., Bailey, A., Nusbaumer, J., Hu, J., Hillman, A., Ornouski, E., Warner, J., Delong, K., 2024. O - Excess in Tropical Cyclones Reflects Local Rain Re - Evaporation More Than Moisture Source Conditions. https://doi.org/10.1029/2023JD039361.

Tian, C., Wang, L., Kaseke, K.F., Bird, B.W., 2018a. Stable isotope compositions (δ2H, δ18O and δ17O) of rainfall and snowfall in the central United States. Sci. Rep. https://doi.org/10.1038/s41598-018-25102-7.

Tian, C., Wang, L., Kaseke, K.F., Bird, B.W., 2018b. Stable isotope compositions (δ2H, δ18O and δ17O) of rainfall and snowfall in the central United States. Sci. Rep. 8, 1–15. https://doi.org/10.1038/s41598-018-25102-7.

Trenberth, K.E., 1999. Atmospheric moisture recycling: Role of advection and local evaporation. J. Clim. 12, 1368–1381. https://doi.org/10.1175/1520-0442(1999)012<1368:AMRROA>2.0.CO;2.

Twidwell, D., Rogers, W.E., Fuhlendorf, S.D., Wonkka, C.L., Engle, D.M., Weir, J.R., Kreuter, U.P., Taylor, C.A., 2013. The rising Great Plains fire campaign: citizens' response to woody plant encroachment. Front. Ecol. Environ. 11. https://doi.org/10.1890/130015.

Van Auken, O.W., 2009. Causes and consequences of woody plant encroachment into western North American grasslands. J. Environ. Manag. 90, 2931–2942. https://doi.org/10.1016/j.jenvman.2009.04.023.

Warner, M.S.C., 2018. Introduction to PySPLIT: A python toolkit for NOAA ARL's HYSPLIT model. Comput. Sci. Eng. 20, 47–62. https://doi.org/10.1109/MCSE.2017.3301549.

Weaver, S.J., Nigam, S., 2011. Recurrent supersynoptic evolution of the great plains low-level Jet. J. Clim. 24, 575–582. https://doi.org/10.1175/2010JCLI3445.1.

Wei, Z., Yoshimura, K., Wang, L., Miralles, D.G., Jasechko, S., Lee, X., 2017. Revisiting the contribution of transpiration to global terrestrial evapotranspiration. Geophys. Res. Lett. 44, 2792–2801. https://doi.org/10.1002/2016GL072235.

Wernli, H., Davies, H.C., 1997. A Lagrangian-based analysis of extratropical cyclones. I: the method and some applications. Q.J.R. Meteorol. Soc. 123, 467–489. https://doi.org/10.1002/qj.49712353811.

Wu, H., Zhang, X., Xiaoyan, L., Li, G., Huang, Y., 2015. Seasonal variations of deuterium and oxygen-18 isotopes and their response to moisture source for precipitation events in the subtropical monsoon region. Hydrol. Process. 29, 90–102. https://doi.org/10.1002/hyp.10132.

Xia, Y., et al., 2009. NLDAS Primary Forcing Data L4 Hourly 0.125 x 0.125 degree V002 [WWW Document]. In: Mocko, David (Ed.), NASA/GSFC/HSL, Greenbelt, Maryland, USA, Goddard Earth Sci. Data Inf. Serv. Cent. (GES DISC). https://doi.org/10.5067/6J5LHHOHZHN4.

Xia, Z., Winnick, M.J., 2021. The competing effects of terrestrial evapotranspiration and raindrop re-evaporation on the deuterium excess of continental precipitation. Earth Planet. Sci. Lett. 572. https://doi.org/10.1016/j.epsl.2021.117120.

Yadava, M.G., Ramesh, R., Pandarinath, K., 2007. A positive 'amount effect' in theSahayadri (Western Ghats) rainfall. Curr. Sci. 93, 560–564.

Yu, W., Guo, R., Thompson, L.G., Zhang, J., Lewis, S., Jing, Z., He, J., Ma, Y., Xu, B., Wu, G., Zhou, X., Tang, W., Wang, Q., Ren, P., Zhang, Z., Qu, D., 2024. Water isotope ratios reflect convection intensity rather than rain type proportions in the pantropics. Sci. Adv. 10. https://doi.org/10.1126/sciadv.ado3258.

Zhang, J., Wang, S., Huang, J., He, Y., Ren, Y., 2023. The precipitation-recycling process enhanced extreme precipitation in Xinjiang, China. Geophys. Res. Lett. 50. https://doi.org/10.1029/2023GL104324.

Zhang, W., Villarini, G., 2019. On the weather types that shape the precipitation patterns across the U.S. Midwest. Clim. Dyn. 53, 4217–4232. https://doi.org/10.1007/s00382-019-04783-4.